# Electrocatalytic performance of oxygen-activated carbon fibre felt anodes mediating degradation mechanism of acetaminophen in aqueous environments

Paweł Jakóbczyk [a,b], Grzegorz Skowierzak [b,c], Iwona Kaczmarzyk [a], Małgorzata Nadolska [a], Anna Wcisło [c], Katarzyna Lota [d], Robert Bogdanowicz [a], Tadeusz Ossowski [b,c], Paweł Rostkowski [e], Grzegorz Lota [d,f], Jacek Ryl [a,*]

[a] *Advanced Materials Center, Gdańsk University of Technology, Narutowicza 11/12, 80-233, Gdańsk, Poland*
[b] *Institute of Biotechnology and Molecular Medicine, Kampinoska 25, 80-180, Gdańsk, Poland*
[c] *Department of Analytical Chemistry, University of Gdansk, Bazynskiego 8, 80-309, Gdansk, Poland*
[d] *Łukasiewicz Research Network – Institute of Non-Ferrous Metals Division in Poznan, Central Laboratory of Batteries and Cells, Forteczna 12, 61-362, Poznan, Poland*
[e] *NILU-Norwegian Institute for Air Research, Instituttveien 18, 2007, Kjeller, Norway*
[f] *Institute of Chemistry and Technical Electrochemistry, Poznan University of Technology, Berdychowo 4, 60–965, Poznan, Poland*

## HIGHLIGHTS

- CFE anodes were modified by thermal, chemical and plasma-chemical methods.
- CFE plasma-chemical treatment had the most efficient electro-oxidation performance.
- Modifications caused minor changes in the specific surface area of CFEs.
- Plasma-treated CFEs shows energy efficiency of 0.073 kWh m$^{-3}$ and rate constant of 1.54 h$^{-1}$.
- High oxidation rates of acetaminophen were attributed to the surface carbonyl species.

## GRAPHICAL ABSTRACT
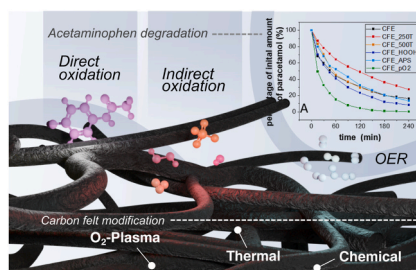
## ABSTRACT

Carbon felts are flexible and scalable, have high specific areas, and are highly conductive materials that fit the requirements for both anodes and cathodes in advanced electrocatalytic processes. Advanced oxidative modification processes (thermal, chemical, and plasma-chemical) were applied to carbon felt anodes to enhance their efficiency towards electro-oxidation. The modification of the porous anodes results in increased kinetics of acetaminophen degradation in aqueous environments. The utilised oxidation techniques deliver single-step, straightforward, eco-friendly, and stable physiochemical reformation of carbon felt surfaces. The modifications caused minor changes in both the specific surface area and total pore volume corresponding with the surface morphology.

A pristine carbon felt electrode was capable of decomposing up to 70% of the acetaminophen in a 240 min electrolysis process, while the oxygen-plasma treated electrode achieved a removal yield of 99.9% estimated utilising HPLC-UV-Vis. Here, the electro-induced incineration kinetics of acetaminophen resulted in a rate constant of 1.54 h$^{-1}$, with the second-best result of 0.59 h$^{-1}$ after oxidation in 30% $H_2O_2$. The kinetics of

\* Corresponding author.
*E-mail address:* jacek.ryl@pg.edu.pl (J. Ryl).

acetaminophen removal was synergistically studied by spectroscopic and electrochemical techniques, revealing various reaction pathways attributed to the formation of intermediate compounds such as *p*-aminophenol and others.

The enhancement of the electrochemical oxidation rates towards acetaminophen was attributed to the appearance of surface carbonyl species. Our results indicate that the best-performing plasma-chemical treated CFE follows a heterogeneous mechanism with only approx. 40% removal due to direct electro-oxidation. The degradation mechanism of acetaminophen at the treated carbon felt anodes was proposed based on the detected intermediate products. Estimation of the cost-effectiveness of removal processes, in terms of energy consumption, was also elaborated. Although the study was focussed on acetaminophen, the achieved results could be adapted to also process emerging, hazardous pollutant groups such as anti-inflammatory pharmaceuticals.

## 1. Introduction

Porous carbon materials such as carbon felt, vitreous carbon, carbon textile, carbon sponge, and carbon fibre can be processed for various applications due to their relatively low cost, good thermal, chemical and mechanical stability, and excellent electrical conductivity. Moreover, porous carbons are well-known for their highly developed surface areas and porosities. The development of pores is significant because it allows carbons to adsorb large quantities of chemicals from gas and liquid phases.

Recently, the most prominent electrode materials are commercially available polyacrylonitrile- or rayon-based carbon felt electrodes (CFEs). CFEs are used due to their good electrical conductivity, high surface area, porosity, ability to provide abundant redox reaction sites, excellent electrolytic efficiency, and mechanical stability at a relatively low cost (González-García et al., 1999; Smith et al., 2015; Huong Le et al., 2017). However, they show poor wettability and low electrochemical activity. Several approaches have been reported in the literature to enhance the electrochemical activity of the felts such as surface modification by plasma (Kahoush et al., 2019), thermal and chemical (Zhou et al., 2014) treatment with the addition of functional groups, and deposition of metal or metal oxides on the electrode surface (Fu et al., 2021; Rahmani et al., 2021). These treatments were efficient in surface modification and functionalisation due to the improved energy efficiency and mechanical properties, increased surface adhesion and affinity towards aqueous solutions. The most commonly used procedure is CFE oxidation, which can be achieved by oxidising acid or thermal treatment. The preferred strategy is a thermal treatment in which the materials are annealed in a furnace fed by a gas flow containing oxygen and/or nitrogen. This activation step may improve the efficiency of the electrochemical processes and wettability through increased oxidised functional groups on the electrode surface. Earlier studies on different CFEs based on a polyacrylonitrile or rayon matrix by thermal treatment at 400 °C for 30 h in air saw significant enhancement of the electrochemical properties of both kinds of CF electrodes (Zhong et al., 1993). However, XPS analysis showed that the rayon-based carbon felts oxidised easier than the polyacrylonitrile-based felts, forming C–O groups on the surface. The microcrystalline structure of the rayon-based felts is assumed to enable broader oxygen interaction with the electrode surface. Moreover, the active electrochemical surface area improved after heat pre-treatment under an $NH_3$ atmosphere at 600 and 900 °C (He et al., 2015). The appearance of nitrogenous groups on the surface increases the number of active sites, improves the wettability, and increases the electrical conductivity. By using thermal treatment of carbon felt under a gas mixture flow of $N_2/O_2$ containing 1% of oxygen at 1000 °C, a porous carbon material was fabricated via the selective etching of amorphous carbon (Le et al., 2016; Orimolade et al., 2020). The thermally obtained porous carbon felt surface and improved hydrophilicity enhanced the electron-transfer efficiency, leading to the development of the electroactive surface area. L. Eifert et al. investigated the influence of chemical and electrochemical ageing by thermal treatment on commercially available polyacrylonitrile- and rayon-based carbon felt electrodes (Eifert et al., 2018). Significant differences were found in how the surface composition, thermal stability and electrochemical behaviour is affected by the different treatment methods.

CFE is an interesting carbonaceous material with a wide range of applications, such as oil/water separation (Cheng et al., 2018; Cao et al., 2020), redox flow batteries (Noh et al., 2017; Lu et al., 2021), electrochemical sensors (Kim et al., 2021), microbial fuel cells (Hidalgo et al., 2016; Kosimaningrum et al., 2021) and water treatment (Zhou et al., 2022), including degradation of pharmaceuticals (Zhou et al., 2014; Le et al., 2016, 2017). Moreover, carbon felt electrodes have been studied as an anode material for the degradation of organic compounds, such as persistent and mobile organic compounds (Zhou et al., 2022), phenol and its derivatives (Kim et al., 2021; Chen et al., 2022), diuron (Rahmani et al., 2021), toluene (Tian et al., 2017),etc.

Plasma treatment surface modification is considered effective and not overly time-consuming, and does not require solvents, so is eco-friendly. In studies, different types of plasma have been used to improve carbon materials' contact angles by using various gases (Hammer et al., 2014). It is known that oxygen plasma forms phenolic and carboxyl functional groups, which significantly influence the hydrophilicity of porous carbon materials and improve the redox activity of these electrodes (Dixon et al., 2016; Ortiz-Ortega et al., 2021). Likewise, nitrogen-carbon functional groups and nitrogen groups (pyrrolic and quaternary nitrogen), formed via surface nitrogen plasma modification, enhance the electron transfer rate and improve the wettability (contact angle <90°) (Huang et al., 2017; Kahoush et al., 2019; Ortiz-Ortega et al., 2021). The physicochemical properties of carbon materials can be easily manipulated through control of the plasma treatment process parameters, opening up possibilities for CFE applications.

Acetaminophen (paracetamol; n-acetyl-*p*-aminophenol) is a widely used analgesic and antipyretic drug. The consumption of acetaminophen is high worldwide because it is cheap, accessible, and available without a prescription. However, acetaminophen readily accumulates in the aquatic environment due to its high solubility and hydrophilicity (Wu et al., 2012). It is currently one of the biggest emerging pollutants worldwide, and it has been detected in various natural matrices, i.e., wastewater, ground, and drinking water (Vieno et al., 2007; Homem and Santos, 2011). This compound reaches the ecosystems in the wild through direct disposal of domestic drugs, discharges of faeces and urine, and inappropriate treatment of industrial effluents. Continuous increases in the concentration of acetaminophen may harm the organisms and the sub-organism level in aquatic environments. The toxicity of acetaminophen for animals and humans is well documented (Brind, 2007). Therefore, effective degradation and removal from the environment are important aspects of animal and human health protection. Conventional wastewater treatments do not always seem to be effective at treating sewage containing pharmaceuticals. It was found that acetaminophen remained in the sewage water after various combinations of conventional treatment, such as coagulation, flocculation, sedimentation, and disinfection by ozone, chlorine, or chlorine dioxide (Benotti et al., 2009). Consequently, the development of effective water treatments enabling the degradation of acetaminophen and other pharmaceuticals is a new challenge for the community. In recent years, many studies have focussed on a cathodic electro-Fenton (EF) process consisting of carbon felt as a viable and effective method for removing

acetaminophen (Le et al., 2016, 2017; Ganiyu et al., 2019; Orimolade et al., 2020). The proposed electrochemical oxidation of acetaminophen mediated by porous carbon felts seems to be a promising alternative to the physicochemical methods used (Arredondo Valdez et al., 2012; Marques et al., 2017).

In this study, for the first time, advanced modification processes (thermal, chemical, and plasma-chemical) were applied to carbon felts towards organic pollutant electro-oxidation. Single-step, low-cost and scalable approaches enabled straightforward and eco-friendly surface modification with the stable performance of the felt surfaces. Our work focussed on CFE activation towards acetaminophen, a reference standard representing anti-inflammatory, organic pharmaceuticals. Carbon felts are flexible and scalable, have high specific areas, and are highly conductive materials that fit the requirements of both anodes and cathodes in advanced electrocatalytic processes.

## 2. Materials and methods

### 2.1. Materials

SIGRACELL® graphite felt (type: GFD 4,6 EA) from SGL Carbon was used for all of the experiments. The EDX spectra of the CFE (Fig. 1c) confirmed the polyacrylonitrile origin, while revealing a small share of Si and Al compounds (<0.8 wt%), plausibly used for impregnation purposes of the product. All reagents used were of analytical grade and were used without further purification. For modification processes, ammonium persulfate (ACS reagent, ≥98%) from Sigma-Aldrich and hydrogen peroxide (30% pure p. a.) from POCH were used. Aqueous solutions of sodium sulphate (≥99%, anhydrous, ACS reagent), and potassium ferricyanide $K_3[Fe(CN)_6]$ (≥99%, anhydrous, ACS reagent) were made with the use of demineralised water. Acetaminophen (European Pharmacopoeia (EP) Reference Standard), *tert*-butyl alcohol (ACS reagent, ≥ 99.0%) were purchased from Aldrich. The highest purity class of oxygen (99.998%) was sourced from Air Liquide.

### 2.2. Electrochemical oxidation setup

The electrochemical oxidation process was carried out in galvanostatic conditions at a current of 200 mA. This type of electrolysis is the easiest to set up as it operates in a two-electrode system. Only the surfaces of the electrodes facing each other are electrochemically active and the electrochemical oxidation takes place there, so two cathodes were used on opposite sides of the anode. The conversion potential (U) is not controlled during galvanostatic electrolysis. This is an advantage of the galvanostatic method because, at a certain point in electrolysis, the mass transport by mixing and diffusion through the electrochemical double layer that is formed at each electrode as a result of electrode polarisation becomes insufficient.

The electrolysis system consists of a 3D-printed polylactic acid (PLA) electrolyser, one anode, and two cathodes. Both of the stainless steel cathodes (ASTM A240, type 316) and the CFE anode were the same dimensions (5 × 6 cm). The thickness of the CFE anode was approx. 4 mm. The CFE anode was positioned in the middle of the reactor, thus, both sides of the electrode were exposed to the treated electrolyte. Two cathodes were applied to achieve symmetric and homogeneous electric field confinement for efficient electrooxidation at both sides of the electrode. Such an approach was used previously by Hilt (2020). Our setup is depicted in Fig. 1a.

A peristaltic pump with a rated flow of 0.2–3000 mL $min^{-1}$; DC power supply (CPX400DP) and a data acquisition system (NI Compact Rio System) were used. The electrolysis process was carried out under ambient conditions (22 °C) for 240 min. The reactive components together at a mixing junction were pumped with a flow rate of 456 mL $min^{-1}$ down a pipe, which provided advantages in the form of faster and safer reactions, cleaner products, and easy scale-up of the electrolyser. Fig. 1 presents the electrolyser setup scheme and SEM/EDX micrographs of the pristine carbon felt surfaces. The topography images of the CFE after each modification are presented in the Supplementary Information file, Figure S1.

### 2.3. Carbon felt electrode modification

Three different CFE modification methodologies of commercially available carbon felts were used. To obtain thermal modification, the carbon felt was heated at 250 or 500 °C with a temperature increase rate of 5 °C $min^{-1}$ in a single-zone horizontal tube furnace PR-90/1300 ITR (Poland). Both processes were conducted for 2 h under an air atmosphere before being cooled to room temperature naturally. These samples were labelled CFE_250T and CFE_500T, respectively. The chemical modifications were performed in hydrogen peroxide (30% $H_2O_2$) or in ammonium persulfate (($NH_4$)$_2$$S_2O_8$), by immersion for 1 h 2 M of ($NH_4$)$_2$$S_2O_8$ was prepared shortly before immersion. The solutions were stirred during the entire process. The samples were named CFE_HOOH and CFE_APS, respectively. After chemical modifications, the activated felts were washed with distilled water. Finally, plasma-chemical modification (CFE_pO2) was performed in a low-pressure plasma system
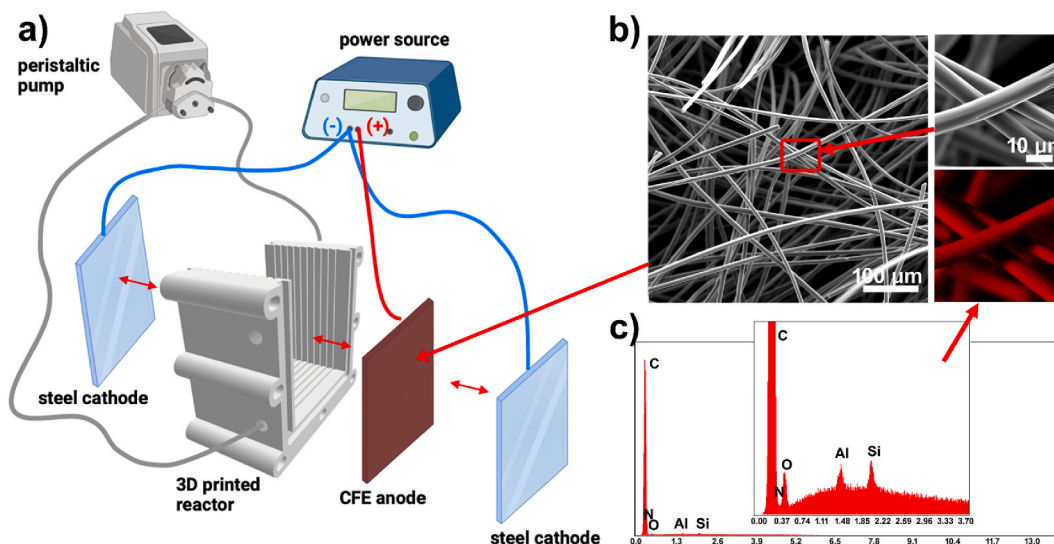


**Fig. 1.** a) Scheme of the electrolyser, b) SEM and EDX micrographs of the carbon felt electrode, c) EDX spectra registered for the CFE before modification.

(Diener Zepto, Germany) for 10 min, exposed to a 300 W oxygen plasma at a frequency of 13.56 MHz. The pressure of the CFE plasma modification was 0.4 mbar and depended on oxygen gas flowing.

### 2.4. Characterisation of carbon felt electrodes

The electrochemical properties of the carbon felt electrodes were measured by a VMP-300 BioLogic potentiostat in a three-electrode cell configuration. The CFEs served as the working electrode. A platinum wire and an Ag/AgCl-coated wire served as the counter and reference electrodes, respectively. The cyclic voltammetry (CV) measurements were conducted in contact with an aqueous 0.5 M $Na_2SO_4$ solution and measured at a sweep rate of 100 mV s$^{-1}$. CVs were also performed in 2.5 mM $K_3[Fe(CN)_6]$ in 0.25 M $Na_2SO_4$ at 100 mV s$^{-1}$. Differential pulse voltammetry (DPV) was performed using a PGStat 302 N potentiostat-galvanostat system (Methrom, Autolab, Netherlands) in the standard three-electrode assembly, where a glassy carbon (GC) electrode served as the working electrode. The active surface area had a circular shape with a diameter of 3 mm. A Pt wire was used as the counter electrode, while Ag/AgCl/3 M KCl was the reference electrode. DPV was carried out between 0 and 0.8 V for the analyte after electrolysis for different amounts of time.

An inverted system was used for High-Performance Liquid Chromatography (HPLC) analysis (Shimadzu LC-20A Series). The column used was a Phenomenex Luna C8 (100 Å, 3 μm, 150 × 4.60 mm). The studies were carried out in a linear solvent gradient (A: $H_2O$ + 0.1% TFA, B: acetonitrile) (0–60% B) for 15 min, in a mobile phase at a flow rate of 1.2 mL min$^{-1}$. Detection was performed with a UV–Vis detector at a wavelength of 243 nm. Prior to the injection, the samples were filtered through a 0.25 μm membrane filter, and separation was carried out at room temperature, 24 ± 1 °C. All UV–Vis spectra acquired without chromatographic separation were recorded in the 210–400 nm range on a PerkinElmer Lambda 40 UV–Vis spectrometer. A 1 cm diameter quartz cuvette microcell was used. All tested samples were diluted 1:10 times with 0.1 M $Na_2SO_4$ solution. The measurements were carried out at a temperature of 25 °C in aqueous solutions of 0.1 M $Na_2SO_4$.

Ultra-high performance liquid chromatography (UHPLC model Vanquish Horizon) coupled with an Orbitrap Q-Exactive-Plus ultrahigh-resolution mass spectrometer (both from ThermoFisher Scientific) were used to analyse the acetaminophen and its transformation products. The mass spectrometer was equipped with a heated electrospray ion source (HESI) that was operated in negative and in positive mode. Chromatographic separation in negative mode was achieved on a Waters® Acquity HSS T3 (100 Å, 1.8 μm, 150 × 2.1 mm) with a gradient of pure water (A) and methanol (B) and with a gradient of 0.1% formic acid in water (A) and acetonitrile (B). Acquisition was carried in full-scan and data-dependent acquisition (top5) modes to facilitate identification of the products and their confirmation. The injection volume was 2 μL.

The TOC studies were performed using a TOC analyser (Shimadzu, Germany). Samples taken from the electrochemical reactor were filtered before analysis and diluted to the measuring range of the TOC analyser.

Scanning electron microscopy (SEM) and energy-dispersive X-ray spectroscopy (EDX) were conducted with a Phenom XL using a 15 kV beam accelerating voltage, working in high vacuum mode, equipped with a SED. The surface chemical composition of the CFEs prior to and after the modification was evaluated using X-ray Photoelectron Spectroscopy (XPS), using high-resolution scans in the *C 1s, O 1s, Si 2p, Al 2p,* and *N 1s* binding energy ranges. An Escalab 250Xi (ThermoFisher Scientific) multispectroscope was utilised, with an Al Kα X-ray source and 650 μm spot diameter. The pass energy was set to 20 eV, scan resolution 0.1 eV. The measurements were carried out under simultaneous low-energy electron and low-energy Ar$^+$ ion bombardment for charge compensation purposes. Finally, the x-axes of the obtained spectra were calibrated to adventitious carbon C 1s at 284.8 eV.

Nitrogen adsorption-desorption isotherms were measured at 77 K (NOVAtouch™ 2, Quantachrome Instruments). Before the

measurements, samples (1 × 3 cm) were degassed at 150 °C for 12 h under a vacuum to remove adsorbed impurities and moisture. The isotherms were analysed with the Quantachrome TouchWin software. The specific surface area ($S_{BET}$) was calculated using the Brunauer-Emmett-Teller (BET) equation in the typical relative pressure range p/p$_0$ from 0.1 to 0.3. The correlation coefficient of the linear regression was not less than 0.99. In addition, the pore volume ($V_{BJH}$) was obtained according to the Barret-Joyner-Halenda (BJH) algorithm.

All contact angle measurements were performed with a Krüss DSA100 goniometer equipped with a CCD camera and connected to a computer with the Advance software. The angle was determined in each case as the mean of the droplets at equilibrium measured on both sides. Each measurement was repeated 20 times. The Young-Laplace method was used to adjust the drop shape (Cirocka et al., 2021; Dąbrowa et al., 2021; Niedziałkowski et al., 2021). Measurements of the dynamics of the change of the contact angle were made using quick measurements taken at an interval of seconds, and the method of adjusting the shape of the droplet below 70° was the height/width method. Measurements of electrolyte wicking through the electrodes over time were performed using 10 mL of 0.1 M $Na_2SO_4$ solution for each sample. Electrode pieces of similar mass were placed gently on the surface of the liquid, and then photos were taken with a camera at various time intervals (5 min, 1, 24 and 72 h).

## 3. Results and discussion

### 3.1. Carbon felt electrodes surface characterisation

The XPS analysis delivered data on the effects of CFE surface modification through different oxidation processes. The spectra recorded in the *C 1s, O 1s,* and *Si 2p* core-level energy ranges are displayed in Fig. 2.

The pristine CFE surface is dominated by aliphatic C–C species (*C 1s* at 284.8 eV), the share of which reaches over 60 at.%. Due to the surface area development of the studied felts, visualised in Fig. 1b, the share of adventitious carbon contaminants may be significant. The presence of the second notable component negatively shifted by approx. −0.8 eV may be related to unsaturated C═C bonds, but also C–Si and C–SiO species. The complex *C 1s* spectra registered for this sample shows various carbon oxidised species. The dominant peak, at 285.5 eV, is related to the presence of hydroxyl and other C–O bonds while the wide peak at higher binding energies is related to C═O, OC═O, NC═O, and
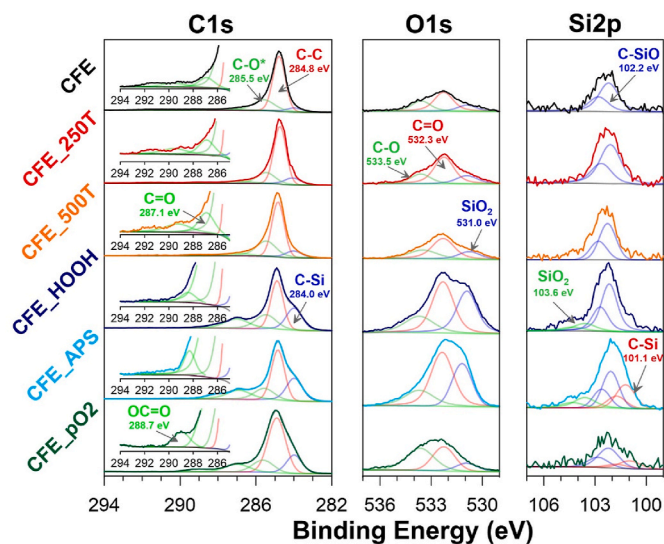


**Fig. 2.** High-resolution XPS spectra recorded in the *C 1s, O 1s,* and *Si 2p* binding energy ranges for CFE samples, with the proposed peak deconvolution model.

similar features. The presence of C–O species on the pristine CFE is due to surface contamination and partial oxidation in the air atmosphere. These results agree with the literature findings (Sobaszek et al., 2016; Ryl et al., 2019; Kunuku et al., 2022). The oxidised to non-oxidised carbon share, $C_{ox} = 0.40$ for pristine CFE, is based on $C\ 1s$ spectral deconvolution.

The analysis and deconvolution of the $O\ 1s$ spectra reveals the presence of not less than three components, most notably peaking at 532.3 eV, an energy characteristic of C=O bonds. Since the share of $C\ 1s$ C=O and OC=O species is negligible in the pristine sample, the signal primarily originates from the adsorbed $CO_2$ from the air and contributes to the presence of adventitious carbon. Other relevant $O\ 1s$ signals include C–O (at 533.5 eV) and C–Si–O (at 531.0 eV) bonds (Kharitonov et al., 2019). Finally, a weak contribution from Si, in the form of a C–Si–O suboxides at 102.2 and 101.1 eV (Wallart et al., 2005; Jung et al., 2016), and $N\ 1s$, in the energy range characteristic of amine C–N bonds (399.6 eV (Niedziałkowski et al., 2021)) were recognised. The detailed results of the deconvolution model are summarised in the Supplementary Information file, Table S2.

CFE modification leads to substantial changes in the surface chemistry but is highly dependent on the proposed approach and the oxidising agent (Klauser et al., 2010; Zielinski et al., 2019). For high-temperature modification in air, the lower studied processing temperature (CFE_250T) was insufficient for a significant shift in the surface chemical composition. Only a small increase in total oxygen content (from 5.3 to 5.6%) was observed with nearly the same $C_{ox} = 0.38$. A small $C_{ox}$ decrease combined with a decrease in the presence of hydroxyl species testifies sample dehydrogenation. Next, increasing the processing temperature to 500 °C (CFE_500T) oxidises the CFE surface, as noted by a significant increase in $C_{ox}$ up to 0.56. This effect is primarily recognised as an increase in C–O and silicon species due to the burnout of carbon material. The latter are present as C–Si–O and O–Si–O ($Si\ 2p_{3/2}$ peak at 103.6 eV).

The chemical oxidation of CFE surfaces, studied after modification in $H_2O_2$ (CFE_HOOH) and $NH_4S_2O_8$ (CFE_APS), is nearly equally effective as high-temperature CFE processing at 500 °C when it comes to carbon species oxidation, offering $C_{ox}$ of 0.63 and 0.55, respectively. However, the chemical nature of the CFEs after oxidation is altered. Unlike high-temperature treatment, the chemically oxidised CFEs are characterised by a major C=O component. Both chemical treatments result in doubling the contribution of the $C\ 1s$ peak at 284.0 eV. Given the nature of the process, the likelihood of C=C bonds formation is low; thus, the most reasonable explanation is the formation of C–Si–O bonds, further confirmed by a threefold increase in the $O\ 1s$ C–Si–O peak contribution at 531.0 eV. An overall increase in total oxygen to 17.4 at.% (from 5.3%), total silicon to 2.5 at.% (from 0.6%), and total nitrogen to 1.5 at. % (from 0.3%) was highest in the case of the CFE_APS sample.

On the other hand, the plasma-chemical oxidation (CFE_pO2 sample) results in, similar to chemical oxidation, carbon chemistry with a significant share in C=O species at the carbon felt surface (11.3 at.% for CFE_pO2 compared to 13.8 and 12.1% for CFE_HOOH and CFE_APS, respectively). However, plasma appears to be less damaging to the carbonaceous framework, as seen by the only small increase in inert Si and N species. Here, the $C_{ox}$ factor is 0.47, which makes it possible to conclude that plasma-chemical treatment is the least invasive, primarily introducing C=O bonds at the carbon felt electrode surface. Neither the pristine sample nor any of the modified CFEs showed a quantitative share of aluminium, unlike the EDX studies (see Fig. 1c), thus suggesting the element is only present in the material volume and absent at the surface.

The specific surface area ($S_{BET}$) and total pore volume ($V_{BJH}$) of the carbon felts before and after surface oxidation using different modification processes were also estimated. It was observed that the modifications caused only minor changes in both the specific surface area and porosity. This result corroborates the SEM images (see the Supplementary Information, Table S3 and Fig. S1, respectively), revealing a similar morphology for all of the samples. The highest values were noted for the thermally treated CFEs, for which the $S_{BET}$ increased up to 28 $m^2\ g^{-1}$ after annealing at 500 °C. On the other hand, the use of ammonium persulfate or oxygen plasma led to a negligible $S_{BET}$ decrease, down to 11 $m^2\ g^{-1}$ (Kopczyński et al., 2017). The $S_{BET}$ for all of the studied electrodes was within one order of magnitude.

The contact angle measurements evaluated the CFEs' hydrophilicity and water volume adsorption. The studied porous electrodes revealed electrolyte permeability and electrochemical parameters. Hence, both the wettability parameter itself and its dynamics become essential. To assess the wettability of the tested materials, measurements were made with the use of water (10 and 100 μL) and 0.1 M $Na_2SO_4$ (10 μL) droplets. The different droplet volumes were to check whether the large mass of the liquid would affect the wettability of a given electrode. The obtained results indicate that it is of importance only in some cases. All of the electrodes are strongly hydrophobic, and their contact angle with water is about 107° (Fig. 3a and b) for a smaller droplet. Increasing the drop to 100 μL resulted in changes in the contact angle of some electrodes. These results are shown in Fig. 3a.

The materials with the highest hydrophobicity were CFE, CFE_250T, and CFE_500T. On the other hand, the CFE_APS and CFE_HOOH electrodes showed more hydrophilic properties. Interestingly, while hydrophobic for small water droplets, the CFE_pO2 electrode absorbed higher droplet volumes completely (see Fig. 3c). This uncommon behaviour may result primarily from interfacial tension and/or altered functionalised surface chemistry of this electrode. The feature remains present when subjected to 0.1 M $Na_2SO_4$ droplets. An interesting exception is the CFE_APS sample, which was highly hydrophilic in contact with water but showed hydrophobicity in contact with the 0.1 M $Na_2SO_4$. Again, this feature was most likely affected by the materials' surface chemistry, their porosity/roughness, and the difference in material surface energy and liquid surface tension. The contact angles in the electrolyte and water did not differ significantly, except for the chemically modified CFEs.

The obtained results seem to confirm the XPS observations regarding the chemistry of the CFEs. The CFE_pO2 and CFE_APS electrodes are both characterised by a higher content of C=O groups, hence their greater hydrophilicity seems to be a rational consequence of this modification. On the other hand, the CFE electrode predominantly contains C–C groups, which results in its high hydrophobicity. The high-thermally treated electrodes (CFE_250T and CFE_500T) still contain a large amount of these groups, and their oxidation degree does not significantly change the hydrophobicity. Nevertheless, we have observed variation of hydrophobicity at chemically oxidised electrodes that contain a large amount of C=O groups. Similar observations were made by other authors (Ifires et al., 2021).

The surface chemistry affects the charge transfer kinetics at the electrode/electrolyte interface, and through electrolyte permeability of the CFEs, the surface area is available for the electro-oxidation process. On the other hand, studying the electrochemical properties addresses the influence of the modification of the CFE on the charge transfer kinetics. The electrochemical window, which for pristine CFE is characterised by a high oxygen evolution potential, is largely affected by the modification procedure. This feature determines the oxidation power in the electrolysis process. The CV analyses of various CFE samples are shown in Fig. 3d. The results show that a few of the studied CFE electrodes were stable to a potential of about 1.3 V vs Ag|AgCl|3 M KCl. The CFE, CFE_250T, CFE_500T, and CFE_APS electrodes had a similar oxygen evolution voltage of about 1.3 V. The carbon felt electrodes modified using hydrogen peroxide (CFE_HOOH), and oxygen plasma (CFE_pO2) had higher oxygen evolution potentials, equal to 1.4 and 1.5 V, respectively, which produced more potent oxidants (Hamdi El Najjar et al., 2014) than the anode with a lower oxygen evolution potential (CFE, CFE_250T, CFE_500T, CFE_APS). The CFE_pO2 sample displays the widest electrochemical window. In contrast, modification by ammonium persulfate led to the development of sizeable double-layer
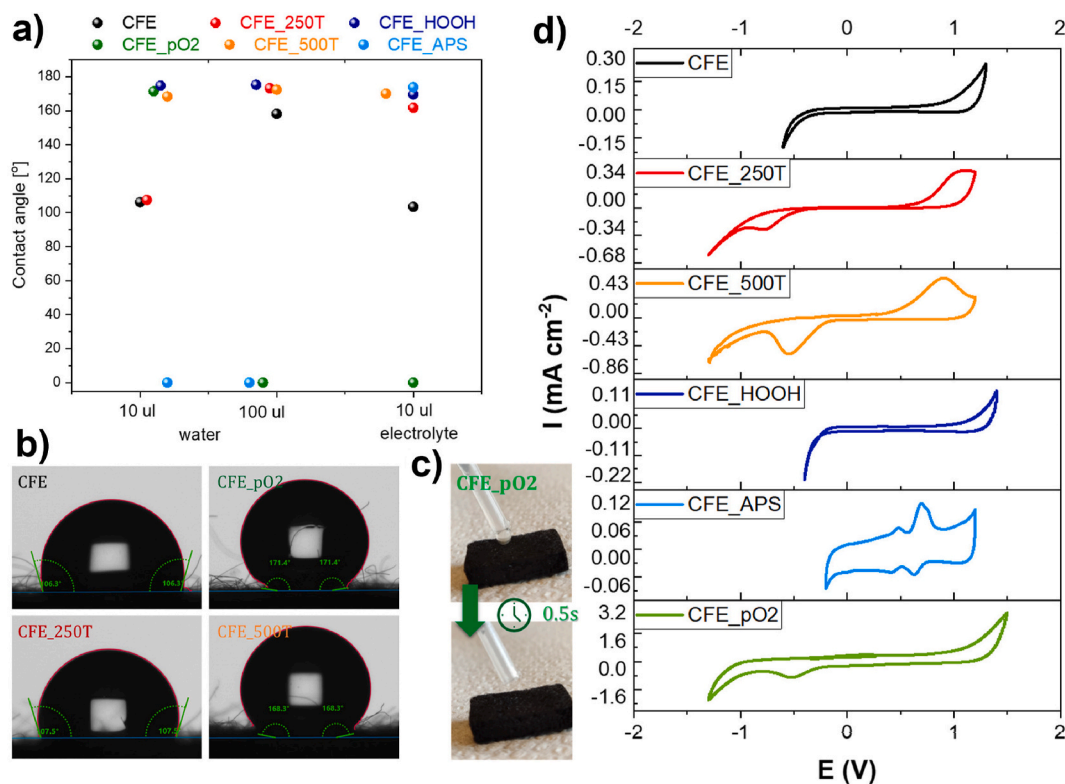
**Fig. 3.** a) contact angle for water (10 and 100 μL) and 0.1 M Na$_2$SO$_4$ (10 μL) droplets; b) photos of CFEs' wettability measurements (WCA, 10 μL sample); c) rapid large water volume adsorption by CFE_pO2 electrode. d) Cyclic voltammogram of pristine CFE and after modifications in 0.5 M Na$_2$SO$_4$ as electrolyte. Scan rate 100 mV s$^{-1}$.

capacitance, causing energy loss and lower current efficiency of electrochemical acetaminophen oxidation. The cathode peak at about −0.5 V is associated with reducing the oxygen that was adsorbed on the electrode surface. The peaks that are present for the CFE_APS are related to ammonium persulfate residuals after chemical modification, which is observed in the SEM images (see the Supplementary Information file, Fig. S1e).

The rate of electrochemical processes is primarily determined by the charge transfer kinetics of the electrochemical oxidation and reduction processes. The CFEs were examined in the presence of ferrocyanides, the most often used redox probe in such studies. These results are presented in the Supplementary Information file Fig. S2a. The obtained data are normalised to the geometric area of the electrode surface. The CVs recorded with the CFEs show the typical feature, i.e., a pair of redox waves centred at about 0.25 V vs. Ag|AgCl, superimposed on the background current attributed to the double-layer capacitance. The peak separation is about 450 mV for the unmodified electrode (CFE), while the lowest and the highest peak separations are 88 and 763 mV for the CFE_HOOH and CFE_250T, respectively. A peak separation in the range between 60 and 210 mV indicates *quasi*-reversible processes for the reversible one-electron-transfer reaction (Ryl et al., 2019; Koterwa et al., 2022).

Chen and McCreery (1996) report that the redox reaction rates for [Fe(CN)$_6$]$^{3-/4-}$ on glassy carbon electrodes do not differ significantly depending on the surface coverage with oxides but are sensitive to single-layer adsorption. Studies on different carbonaceous materials show that various oxidation treatments may alter electrode surface termination and that, as a result, electron transfer is altered (Wang et al., 2009; Ryl et al., 2019; Zielinski et al., 2019). This shows the effect of surface termination on the charge transfer kinetics. However, in our study, the correlation between the peak separation value and the number of functional groups on the surface is unclear. The surface analysis and dependence on electrochemistry are more convenient for flat electrodes. The surface geometry factor and its complexity have too much influence on the peak separation value obtained.

We also studied the acetaminophen oxidation reaction in the supporting electrolyte. The results are summarised in the Supplementary Information file, Fig. S2b. Higher acetaminophen oxidation peaks indicate a larger electrochemical active electrode area (EASA) involved in the electro-oxidation reaction of acetaminophen. The CV oxidation of acetaminophen correlated with the CV of the electrodes in pure supporting electrolytes gives us a better understanding of the electrochemical properties of the electrodes. It must also be said that for the degradation of organic compounds, both direct and indirect oxidation processes must be considered. Hence, the lowest peak separation is not always the best. A large peak separation and peak shifts indicate the complexity of the electrode structure and, in some cases, better wettability. When the wettability is poor, the electrode resembles a flat electrode rather than a porous one.

### 3.2. Acetaminophen electrochemical oxidation (EO) tests

During the electrochemical oxidation tests, to ensure a current flow of 200 mA, the galvanostat increased the applied voltage. Thanks to this, the electrolysis continued and another substance with the lowest redox potential underwent electrolysis (Hilt, 2020). The electrolysis was performed at a neutral pH in 0.1 M Na$_2$SO$_4$. The current for the galvanostatic oxidation of acetaminophen was selected based on the obtained current-voltage relationship ranging from 0.0 to 6.5 V in a two-electrode system. In the Supplementary Information file, Fig. S3, we can see an acetaminophen oxidation peak of about 2.25 V followed by an increase in currents at a potential of about 3.5 V due to the decomposition of water. Therefore, the current selected for the electrochemical oxidation of acetaminophen is lower than for water decomposition and high enough to oxidise acetaminophen. This avoids the electrode getting blocked by gases generated during water decomposition and eliminates

energy losses due to water decomposition.

The amount of energy consumed (EC) during the electrolysis can be calculated based on the recorded chronoamperometry curves (Fig. 4a). This is projected in Table 1. Different potentials indicate different electrode resistances, active surface areas and/or difficulties in mass transfer in the electrode layer during the electrolysis process. One can see in Fig. 4a that this potential changes over time. We can observe two types of curves, the first where the potential increases gradually (curve for CFE_pO2) while abrupt potential changes characterise the second type for the remaining electrodes. The difference in potential changes may result from the electrodes' different wettability and water sorption. The gradual increase of the CFE_pO2 potential may be associated with the difficulty in transporting the mass of electroactive substances to the electrode surface due to the depletion of the oxidised compound and the formation of an electrical double layer at the surface of polarised electrodes. In the case of the remaining electrodes (CFE, CFE_250T, CFE_500T, CFE_HOOH, CFE_APS), the surface underwent modification after a certain time (the flat part of the curve up to 60 min for CFE_500T in Fig. 4a). The length of this transition process depended on the CFE surface area development, as determined by the BET method. The longest initial transition (60 min) was recorded for the CFE_500T, which showed the largest area (28 m$^2$), while the CFE_APS and CFE were characterised by shorter transition lengths (35 min). After changing the properties to hydrophilic, a more intensified electrolysis process (potential increase) followed, which involved electrode polarisation and a change in the number of electroactive compounds in the layer close to the electrode, affecting the impediment to mass transfer and the increase of potential. Next, the process stabilised at a higher potential.

The electrodes underwent the wetting process with different dynamics, thus passing the electrolyte to a different degree. This process was further affected by the CFE oxidation induced by electrolysis. CFEs of similar mass were immersed in an electrolyte (10 mL), and then their flotation or sedimentation was observed over time. Initially, all but two of the CFEs floated on the surface. The CFE_pO2 electrode immediately sank to the bottom, and the CFE_APS floated just below the electrolyte surface (Fig. 4b). On the other hand, the majority of the electrodes subjected to the electrolysis for over 1 h sank beneath the electrolyte surface, but the CFE_500T, like the CFE_pO2, sank to the bottom almost immediately (Fig. 5c), and the CFE, CFE_HOOH electrodes only after about a day. Keeping the electrodes in the electrolyte for a prolonged period (up to three days) caused their swelling. Supporting contact angle measurements after the electrolysis are summarised in the Supplementary Information file Fig. S4.

Four complementary techniques were used to determine the efficiency of acetaminophen oxidation by electrolysis: electrochemical (CV and DPV), UV–Vis and HPLC-UV-Vis. The initial acetaminophen concentration in the electrolyte was 200 mg L$^{-1}$. A 240-min-long treatment

**Table 1**

Remaining acetaminophen content after 240 min of electrolysis (galvanostatic oxidation), determined using HPLC, DPV, CV, and UV, together with energy consumption at the end of the process and EE of acetaminophen removal.

| Electrode | Acetaminophen content/% | | | | EC$_{240\ min}$ kWh m$^{-3}$ | EE$_{1\%\ removal}$ kWh m$^{-3}$ |
|---|---|---|---|---|---|---|
| | HPLC-UV-Vis | UV | DPV | CV | | |
| CFE | 16.1 | 9.7 | 22.8 | 23.6 | 7.47 | 0.09 |
| CFE_250T | 27.4 | 22.4 | 32.4 | 32.4 | 7.91 | 0.11 |
| CFE_500T | 17.1 | 21.4 | 23.6 | 23.6 | 7.31 | 0.09 |
| CFE_HOOH | 8.3 | 5.4 | 20.0 | 14.3 | 7.70 | 0.08 |
| CFE_APS | 13.4 | 29.0 | 18.8 | 18.4 | 9.05 | 0.10 |
| CFE_pO2 | 0.1 | 11.2 | 7.4 | 7.1 | 7.32 | 0.07 |

made it possible to draw conclusions on the efficiency of each proposed surface modification on the acetaminophen removal rate. While all of the electrodes were capable of decomposing over 70% of the acetaminophen in the electrolyte, the lowest yield was observed for the CFE_250T (27.4% remained as confirmed by HPLC-UV-Vis), while the CFE_pO2 had the higher removal yield (0.1% remained). Here, the acetaminophen was almost completely removed.

The dynamics of acetaminophen removal through the experiment (based on HPLC-UV-Vis measurements) are visualised in Fig. 5a. The acetaminophen electro-oxidation rate constant $k$ was determined based on the relationship between the acetaminophen concentration remaining throughout the electrolysis to the initial concentration, Eq. (1):

$$ln\left(\frac{C_{(t)}}{C_0}\right) = kt \tag{1}$$

where $t$ is the electrolysis duration. The function is visualised in the Supplementary Information file, Fig. S5. The linear relationship obtained indicates a first-order reaction. The highest constant rate was 1.54 h$^{-1}$ for the CFE_pO2 and was over several times higher than for the others i.e., 0.42 (unmodified CFE), 0.31 (CFE_250T), 0.43 (CFE_500T), 0.59 (CFE_HOOH) and 0.48 (CFE_APS).

In Fig. 5b–e, the process of the acetaminophen removal for the most efficient CFE_pO2 electrode is determined. An improvement over the initial electrode can be observed for the chemical modifications, particularly for the modification with hydrogen peroxide where the acetaminophen content after 240 min equals 8.3 in relation to 16.1% after electrolysis using the pristine electrode (CFE). The electrode modified with oxygen plasma (CFE_pO2) is also the best electrode due to its energy efficiency for acetaminophen decomposition. The acetaminophen content, together with energy consumption (EC) and energy efficiencies for 1% acetaminophen removal (EE) for electrolysis using different CFEs are summarised in Table 1. The reasonable energy efficiency of the removal using pristine CFE, compared to other treatments,
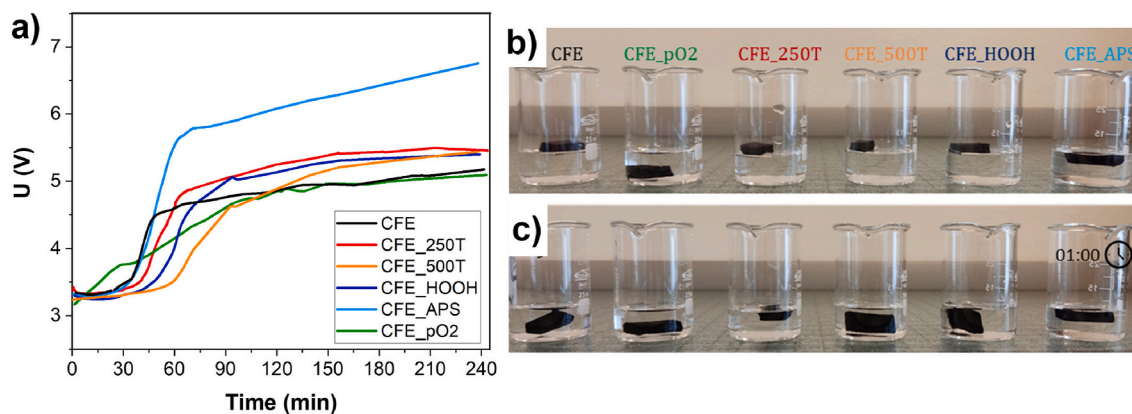


**Fig. 4.** a) Changes of voltage during acetaminophen electrochemical oxidation in 0.1 M Na$_2$SO$_4$ at 200 mA for the carbon felt electrode and its modifications; CFE photos immersed in 0.1 M Na2SO4 b) before and c) after the electrolysis.
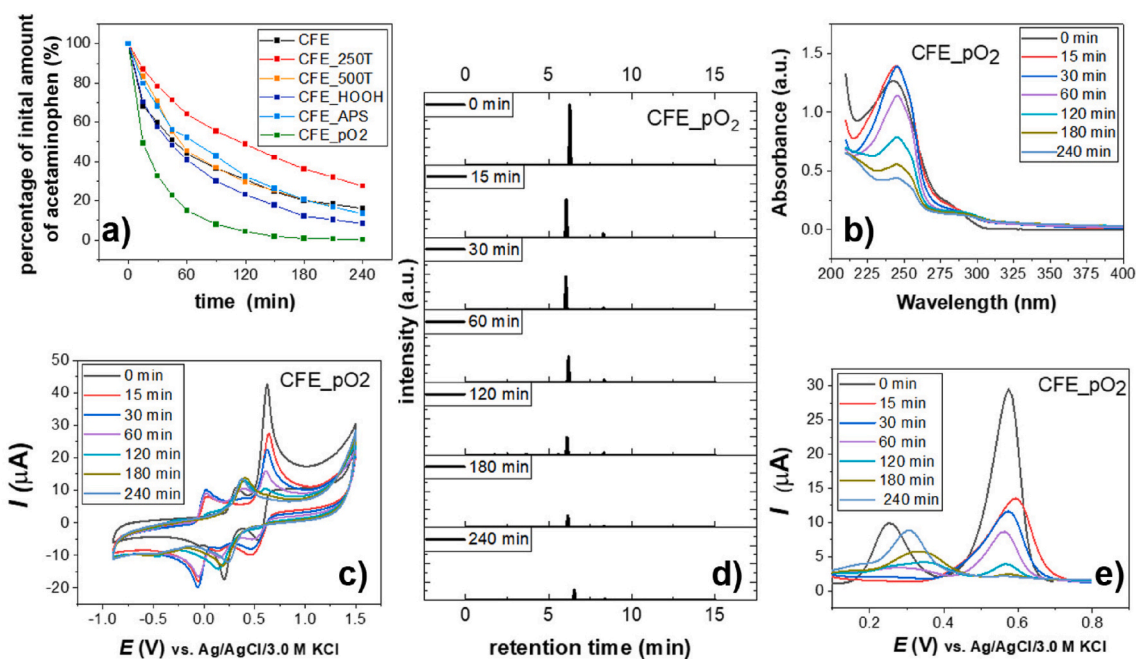
**Fig. 5.** a) Acetaminophen content analysis using HPLC-UV-Vis method during electrolysis on pristine carbon felt (CFE) and after thermal (CFE_250T, CFE_500T), chemical (CFE_HOOH, CFE_APS) and chemical-plasma (CFE_pO2) modification; b) UV–Vis, c) CV, d) HPLC-UV-Vis, and e) DPV curves registered during electrolysis on the chemical-plasma-modified carbon felt (CFE_pO2).

is explained by the formation of carbonyl species under the electro-oxidation process. The XPS data is shown in the Supplementary Information file, Fig. S6, and Table S2.

As can be seen in Table 1, the obtained results often differ from each other. This is due to the fundamental differences in the methodologies of the chosen analytical techniques when studying complex mixtures of substances. The electrochemical methods such as cyclic voltammetry and differential pulse voltammetry were found to be less suitable and produced larger experimental errors. On the other hand, the carbon released from the electrode affects the shift of the UV–Vis spectrum, causing additional peaks and making the interpretation difficult. HPLC-UV-Vis seems to be the most accurate method in this case.

The HPLC-UV-Vis, UV–Vis, CV, and DPV curves for the remaining carbon felts (CFE, CFE_250T, CFE_500T, CFE_HOOH, CFE_APS) are shown in the Supplementary Information file, Figs. S7–S10. The HPLC-UV-Vis studies of acetaminophen oxidation made it possible to determine the concentration of acetaminophen and intermediates that were formed in the reaction (Fig. 5d and S7). Peaks for different retention times were noted (5.5, 6, 8.3 min), confirming the presence of various compounds during electrolysis and their disappearance with the duration of the electrochemical oxidation process. The HPLC reports of Periyasamy (Periyasamy and Muthuchamy, 2018) reveal that the primary acetaminophen electrolysis intermediates are benzoquinone, hydroquinone, and carboxylic acids. The results of qualitative analyses with UHPLC-Orbitrap-HRAM-MS revealed a more detailed list of intermediates, including *p*-aminophenol, and several other molecules reported in the literature (Hamdi El Najjar et al., 2014; López Zavala and Jaber Lara, 2018; Benssassi et al., 2021), which are listed in detail in the Supplementary Information file, Figure S11.

Changes were also observed in the UV–Vis spectra absorbance of acetaminophen (Fig. 5b and S8). Moctezuma et al. (2012) reported two characteristic absorption bands for acetaminophen, with a maximum at 208 and 243 nm associated with $\pi$-$\pi^*$ transition and the latter n-$\pi^*$ transition of the C=O group. In our case, the observed absorbance peak occurs at 243 nm, and decreases with the increasing electrolysis duration. The decrease in the concentration of acetaminophen is faster than the decrease in the absorbance intensity, which is related to the

formation of the intermediates (benzoquinone) during the reaction process (Brillas et al., 2005; de Luna et al., 2012; Moctezuma et al., 2012). Apart from the decrease in absorption intensity due to the decomposition of acetaminophen, an increase in absorption was observed in the range of 280–310 nm, associated with the formation of hydroquinone (Moctezuma et al., 2012).

The CV curves in Fig. 5c and S9 reveal an acetaminophen oxidation peak at about 0.6 V and a reduction peak at around 0.3 V vs. Ag|AgCl. The position of the anodic peak is affected by the concentration of acetaminophen during the electrolysis (Berte et al., 2016). The solution taken for the tests during the electrolysis shows additional reduction peaks at −0.05, −0.25, and −0.65 V, as well as oxidation peaks between 0.3 and 0.4 V and at about 0.0 V vs. Ag|AgCl, all of which are associated with acetaminophen intermediate decomposition products, such as benzoquinone, hydroquinone and carboxylic acids (Periyasamy and Muthuchamy, 2018). On the other hand, the DPV studies do not show such complexity of the reaction mixture due to the limitation of the measurement range (Fig. 5e and S10).

Three competing oxidation processes occur throughout the electrolysis carried out at the carbon felt electrodes, namely: (I) direct acetaminophen oxidation with the formation of benzoquinone and hydroxyquinone as the primary intermediates; (II) production of free radicals inducing indirect acetaminophen oxidation; and (III) the oxygen evolution reaction (OER) process. These reaction pathways are illustrated in Fig. 6.

To further study the role of the formation of hydroxyl radicals in the electrocatalytic acetaminophen removal, another experiment was proposed and conducted with the use of the best-performing CFE_pO2 electrode. *Tert*-Butyl alcohol (1 M) was added during the electrolysis process as the scavenger of hydroxyl radicals (Liu et al., 2019). Its influence on the acetaminophen electro-oxidation is presented in the Supplementary Information file, Figure S12. The acetaminophen removal rate at the CFE_pO2 in the presence of the scavenger reached approx. 40% within 240 min of electrolysis, compared to over 99% as initially reported with HPLC-UV-Vis. The total organic content (TOC) of the same two electrolytes was also measured. This measurement, presented in the Supplementary Information file, Figure S13, reveals a
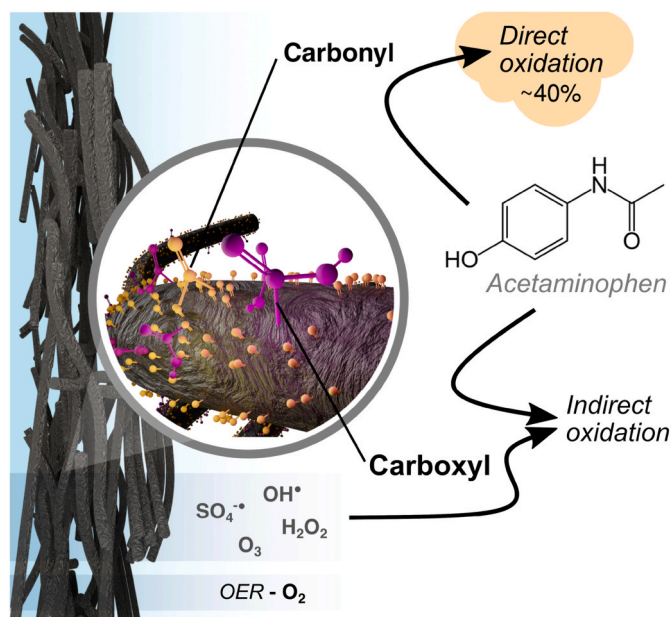
**Fig. 6.** Scheme presenting various oxidation processes taking place at CFE surface.

similar trend to that observed for the HPLC-UV-Vis analysis, but with lower electro-oxidation yields. The outcome can be explained by the incomplete electro-oxidation of acetaminophen by-products but also by the presence of other organic contaminants, such as limited dissolution of the CFE electrodes or hydrolysis of the PLA electrolyser walls. It should also be noted that the presence of a scavenger (*t*-butyl alcohol) increases the content of total carbon in the electrolyte compared to the solutions in which there was no scavenger.

The above experiments clearly demonstrated that the acetaminophen removal follows a heterogeneous electro-oxidation mechanism, with the formation of hydroxyl radicals as the main driving force under the studied conditions. It is worth noting that persulfate or sulphate radicals generated due to the use of sulphates as the supporting electrolyte may also play a role in the degradation process (Divyapriya and Nidheesh, 2021).

As observed earlier, acetaminophen electro-oxidation is competitive with OER, thus increasing the overpotential of the latter process will improve the energy efficiency of the former. The two highest OER potentials were observed after CFE modification by oxygen plasma and $H_2O_2$, reaching 1.5 and 1.4 V, respectively. The plasma-chemical oxidation shows the best acetaminophen oxidation rate constant, far superior to any other CFE modification, again seconded by $H_2O_2$ modification. In both cases, the CFE surface chemistry is characterised by the highest content of carbonyl species, while the XPS results suggest that the plasma is less damaging to the carbonaceous framework. Carbonyl functional groups are related to the more hydrophilic surfaces of the CFEs, thus enhancing the wettability and absorption of the electrolyte by the electrode (Xue et al., 2015; Zhu et al., 2021). Moreover, the presence of this specific functionalisation has a notable impact on the direct acetaminophen electro-oxidation pathway by reducing the anodic activation overpotentials. This is due to the protonation of surface carbonyl groups on oxidation with O atoms bearing a positive charge (Di Corcia et al., 1993; Xue et al., 2015). Next, the carbonyl O pulls the electronic density of π bonds, moving the positive charge towards the carbonyl C atoms and making them strong electrophiles, which are subject to attack by nucleophilic acetaminophen molecules.

## 4. Conclusions

In summary, we have shown the electrocatalytic performance of

oxygen-activated carbon fibre felt anodes modified by advanced processes (thermal, chemical, and plasma-chemical) inducing oxygen-rich surficial groups such as carboxyls and carbonyls. Surficial groups significantly modify the felt wetting revealing the highest hydrophobicity of the thermally treated samples, while the chemically modified surfaces are hydrophilic. The plasma-treated felts display hydrophilic performance, instantly absorbing larger droplets. This effect was attributed to the interfacial tension of the sample's surface. The oxygen plasma also induces the widest electrochemical window and higher oxygen evolution potentials than other modification processes allowing more potent oxidants (i.e. OH-, $SO_4^{2-}$, $H_2O_2$ and $O_3$) to form. Each modification process induces different electrocatalytic performance of the felt anodes mediating the degradation mechanism of acetaminophen conducted in aqueous environments. Formation of carbonyl species at pristine CFE surface was also observed during electro-oxidation process.

The electrolysis decomposition efficiency of acetaminophen was revealed by HPLC-UV-Vis studies indicating that the plasma-modified anodes resulted in the most efficient process. We stated that oxygen plasma soaking in a water solution provides improved contact with the electrolyte and more effective electro-oxidation of organic compounds. The competing oxidation processes depend on the applied modification, changing the impact of specific mechanisms such as direct and indirect acetaminophen oxidation or oxygen evolution reaction. The studies on the best performing electrode, CFE_pO2, in the presence of *Tert*-Butyl alcohol as a scavenger revealed that acetaminophen removal follows a heterogeneous electro-oxidation mechanism with the formation of hydroxyl radicals as the main driving force under the studied conditions. Formation of *p*-aminophenol and several other intermediates were observed with UHPLC-Orbitram-HRAM-MS.

Given the low-cost and good performance in sorption and electrocatalytic performance, carbon fibre felt can be considered as an anode for organic pollutant electro-oxidation where their properties can be tuned by single-step, eco-friendly modifications.

## CRediT author statement

Conceptualization: J.R., P.J. and R.B., Methodology: P.J. and T.O., Validation: P.J. and G.S., Formal analysis: P.J., Investigation: P.J., G.S., I·K., M.N., A.W., P.R. and J.R., Resources: K.L. and G.L., Data curation: G.S. and J.R., Writing – Original Draft: P.J, I·K., M.N., A.W., K.L, R.B., P. R. and J.R., Writing – Review & Editing: R.B., T.O., G.L. and J.R., Visualization: P.J. and J.R., Supervision: J.R. and R.B., Project administration J.R., Funding acquisition T.O. and R.B.

## Declaration of competing interest

The authors declare that they have no known competing financial interests or personal relationships that could have appeared to influence the work reported in this paper.

## Data availability

Data will be made available on request.

## Appendix A. Supplementary data

Supplementary data to this article can be found online at https://doi. org/10.1016/j.chemosphere.2022.135381.

# References

Arredondo Valdez, H.C., García Jiménez, G., Gutiérrez Granados, S., Ponce de León, C., 2012. Degradation of paracetamol by advance oxidation processes using modified reticulated vitreous carbon electrodes with $TiO_2$ and $CuO/TiO_2/Al_2O_3$. Chemosphere 89, 1195–1201. https://doi.org/10.1016/j.chemosphere.2012.07.020.

Benotti, M.J., Trenholm, R.A., Vanderford, B.J., Holady, J.C., Stanford, B.D., Snyder, S. A., 2009. Pharmaceuticals and endocrine disrupting compounds in U.S. Drinking water. Environ. Sci. Technol. 43, 597–603. https://doi.org/10.1021/es801845a.

Benssassi, M.E., Mammeri, L., Talbi, K., Lekikot, B., Sehili, T., Santaballa, J.A., Canle, M., 2021. Removal of paracetamol in the presence of iron(III) complexes of glutamic and lactic acid in aqueous solution under NUV irradiation. Separ. Purif. Technol. 261, 118195 https://doi.org/10.1016/j.seppur.2020.118195.

Berte, M., Appia, F., Sanogo, I., Ouattara, L., 2016. Electrochemical oxidation of the paracetamol in its commercial formulation on platinum and ruthenium dioxide electrodes. Int. J. Electrochem. Soc. 11, 7736–7749. https://doi.org/10.20964/2016.09.44.

Brillas, E., Sirés, I., Arias, C., Cabot, P.L., Centellas, F., Rodríguez, R.M., Garrido, J.A., 2005. Mineralization of paracetamol in aqueous medium by anodic oxidation with a boron-doped diamond electrode. Chemosphere 58, 399–406. https://doi.org/10.1016/j.chemosphere.2004.09.028.

Brind, A.M., 2007. Drugs that damage the liver. Medicine 35, 26–30. https://doi.org/10.1053/j.mpmed.2006.10.005.

Cao, N., Guo, J., Cai, K., Xue, Q., Zhu, L., Shao, Q., Gu, X., Zang, X., 2020. Functionalized carbon fiber felts with selective superwettability and fire retardancy: designed for efficient oil/water separation. Separ. Purif. Technol. 251, 117308 https://doi.org/10.1016/j.seppur.2020.117308.

Chen, P., McCreery, R.L., 1996. Control of electron transfer kinetics at glassy carbon electrodes by specific surface modification. Anal. Chem. 68, 3958–3965. https://doi.org/10.1021/ac960492r.

Chen, S., Chu, X., Wu, L., Foord, J.S., Hu, J., Hou, H., Yang, J., 2022. Three-Dimensional $PbO_2$-modified carbon felt electrode for efficient electrocatalytic oxidation of phenol characterized with in situ ATR-FTIR. J. Phys. Chem. C 126, 912–921. https://doi.org/10.1021/acs.jpcc.1c07444.

Cheng, Y., He, G., Barras, A., Coffinier, Y., Lu, S., Xu, W., Szunerits, S., Boukherroub, R., 2018. One-step immersion for fabrication of superhydrophobic/superoleophilic carbon felts with fire resistance: fast separation and removal of oil from water. Chem. Eng. J. 331, 372–382. https://doi.org/10.1016/j.cej.2017.08.088.

Cirocka, A., Zarzeczańska, D., Wcisło, A., 2021. Good choice of electrode material as the key to creating electrochemical sensors—characteristics of carbon materials and transparent conductive oxides (TCO). Materials 14, 4743. https://doi.org/10.3390/ma14164743.

Dąbrowa, T., Wcisło, A., Majstrzyk, W., Niedziałkowski, P., Ossowski, T., Więckiewicz, W., Gotszalk, T., 2021. Adhesion as a component of retention force of overdenture prostheses-study on selected Au based dental materials used for telescopic crowns using atomic force microscopy and contact angle techniques. J. Mech. Behav. Biomed. Mater. 121, 104648 https://doi.org/10.1016/j.jmbbm.2021.104648.

de Luna, M.D.G., Veciana, M.L., Su, C.-C., Lu, M.-C., 2012. Acetaminophen degradation by electro-Fenton and photoelectro-Fenton using a double cathode electrochemical cell. J. Hazard Mater. 217–218, 200–207. https://doi.org/10.1016/j.jhazmat.2012.03.018.

Di Corcia, A., Marchese, S., Samperi, R., 1993. Evaluation of graphitized carbon black as a selective adsorbent for extracting acidic organic compounds from water. J. Chromatogr. A 642, 163–174. https://doi.org/10.1016/0021-9673(93)80084-L.

Divyapriya, G., Nidheesh, P.V., 2021. Electrochemically generated sulfate radicals by boron doped diamond and its environmental applications. Curr. Opin. Solid State Mater. Sci. 25, 100921 https://doi.org/10.1016/j.cossms.2021.100921.

Dixon, D., Babu, D.J., Langner, J., Bruns, M., Pfaffmann, L., Bhaskar, A., Schneider, J.J., Scheiba, F., Ehrenberg, H., 2016. Effect of oxygen plasma treatment on the electrochemical performance of the rayon and polyacrylonitrile based carbon felt for the vanadium redox flow battery application. J. Power Sources 332, 240–248. https://doi.org/10.1016/j.jpowsour.2016.09.070.

Eifert, L., Banerjee, R., Jusys, Z., Zeis, R., 2018. Characterization of carbon felt electrodes for vanadium redox flow batteries: impact of treatment methods. J. Electrochem. Soc. 165, A2577–A2586. https://doi.org/10.1149/2.0531811jes.

Fu, W., Du, X., Su, P., Zhang, Q., Zhou, M., 2021. Synergistic effect of Co(III) and Co(II) in a 3D structured $Co_3O_4$/carbon felt electrode for enhanced electrochemical nitrate reduction reaction. ACS Appl. Mater. Interfaces 13, 28348–28358. https://doi.org/10.1021/acsami.1c07063.

Ganiyu, S.O., Oturan, N., Raffy, S., Cretin, M., Causserand, C., Oturan, M.A., 2019. Efficiency of plasma elaborated sub-stoichiometric titanium oxide (Ti4O7) ceramic electrode for advanced electrochemical degradation of paracetamol in different electrolyte media. Separ. Purif. Technol. 208, 142–152. https://doi.org/10.1016/j.seppur.2018.03.076.

González-García, J., Bonete, P., Expósito, E., Montiel, V., Aldaz, A., Torregrosa-Maciá, R., 1999. Characterization of a carbon felt electrode: structural and physical properties. J. Mater. Chem. 9, 419–426. https://doi.org/10.1039/a805823g.

Hamdi El Najjar, N., Touffet, A., Deborde, M., Journel, R., Karpel Vel Leitner, N., 2014. Kinetics of paracetamol oxidation by ozone and hydroxyl radicals, formation of transformation products and toxicity. Separ. Purif. Technol. 136, 137–143. https://doi.org/10.1016/j.seppur.2014.09.004.

Hammer, E.-M., Berger, B., Komsiyska, L., 2014. Improvement of the performance of graphite felt electrodes for vanadium-redox-flow-batteries by plasma treatment. Int. J. Renew. Energy Dev. 3, 7–12. https://doi.org/10.14710/ijred.3.1.7-12.

He, Zhangxing, Shi, L., Shen, J., He, Zhen, Liu, S., 2015. Effects of nitrogen doping on the electrochemical performance of graphite felts for vanadium redox flow batteries: nitrogen-doped graphite felt for vanadium redox flow batteries. Int. J. Energy Res. 39, 709–716. https://doi.org/10.1002/er.3291.

Hidalgo, D., Tommasi, T., Bocchini, S., Chiolerio, A., Chiodoni, A., Mazzarino, I., Ruggeri, B., 2016. Surface modification of commercial carbon felt used as anode for Microbial Fuel Cells. Energy 99, 193–201. https://doi.org/10.1016/j.energy.2016.01.039.

Hilt, G., 2020. Basic strategies and types of applications in organic electrochemistry. Chemelectrochem 7, 395–405. https://doi.org/10.1002/celc.201901799.

Homem, V., Santos, L., 2011. Degradation and removal methods of antibiotics from aqueous matrices – a review. J. Environ. Manag. 92, 2304–2347. https://doi.org/10.1016/j.jenvman.2011.05.023.

Huang, Y., Deng, Q., Wu, X., Wang, S., 2017. N, O Co-doped carbon felt for high-performance all-vanadium redox flow battery. Int. J. Hydrog. 42, 7177–7185. https://doi.org/10.1016/j.ijhydene.2016.04.004.

Huong Le, T.X., Bechelany, M., Cretin, M., 2017. Carbon felt based-electrodes for energy and environmental applications: a review. Carbon 122, 564–591. https://doi.org/10.1016/j.carbon.2017.06.078.

Ifires, M., Addad, A., Barras, A., Hadjersi, T., Chegroune, R., Szunerits, S., Boukherroub, R., Amin, M.A., 2021. Cathodic pre-polarization studies on the carbon felt/KOH interface: an efficient metal-free electrocatalyst for hydrogen generation. Electrochim. Acta 375, 137981. https://doi.org/10.1016/j.electacta.2021.137981.

Jung, H., Kim, W.-H., Oh, I.-K., Lee, C.-W., Lansalot-Matras, C., Lee, S.J., Myoung, J.-M., Lee, H.-B.-R., Kim, H., 2016. Growth characteristics and electrical properties of $SiO_2$ thin films prepared using plasma-enhanced atomic layer deposition and chemical vapor deposition with an aminosilane precursor. J. Mater. Sci. 51, 5082–5091. https://doi.org/10.1007/s10853-016-9811-0.

Kahoush, M., Behary, N., Cayla, A., Mutel, B., Guan, J., Nierstrasz, V., 2019. Surface modification of carbon felt by cold remote plasma for glucose oxidase enzyme immobilization. Appl. Surf. Sci. 476, 1016–1024. https://doi.org/10.1016/j.apsusc.2019.01.155.

Kharitonov, D.S., Sommertune, J., Örnek, C., Ryl, J., Kurilo, I.I., Claesson, P.M., Pan, J., 2019. Corrosion inhibition of aluminium alloy AA6063-T5 by vanadates: local surface chemical events elucidated by confocal Raman micro-spectroscopy. Corrosion Sci. 148, 237–250. https://doi.org/10.1016/j.corsci.2018.12.011.

Kim, M., Song, Y.E., Xiong, J.-Q., Kim, K.-Y., Jang, M., Jeon, B.-H., Kim, J.R., 2021. Electrochemical detection and simultaneous removal of endocrine disruptor, bisphenol A using a carbon felt electrode. J. Electroanal. Chem. 880, 114907 https://doi.org/10.1016/j.jelechem.2020.114907.

Klauser, F., Ghodbane, S., Boukherroub, R., Szunerits, S., Steinmüller-Nethl, D., Bertel, E., Memmel, N., 2010. Comparison of different oxidation techniques on single-crystal and nanocrystalline diamond surfaces. Diam. Relat. Mater. 19, 474–478. https://doi.org/10.1016/j.diamond.2009.11.013.

Kopczyński, K., Pęziak-Kowalska, D., Lota, K., Buchwald, T., Parus, A., Lota, G., 2017. Persulfate treatment as a method of modifying carbon electrode material for aqueous electrochemical capacitors. J. Solid State Electrochem. 21, 1079–1088. https://doi.org/10.1007/s10008-016-3452-8.

Kosimaningrum, W.E., Ouis, M., Holade, Y., Buchari, B., Noviandri, I., Kameche, M., Cretin, M., Innocent, C., 2021. Platinum nanoarrays directly grown onto a 3D-carbon felt electrode as a bifunctional material for garden compost microbial fuel cell. J. Electrochem. Soc. 168, 025501 https://doi.org/10.1149/1945-7111/abde7c.

Koterwa, A., Kaczmarzyk, I., Mania, S., Cieslik, M., Tylingo, R., Ossowski, T., Bogdanowicz, R., Niedziałkowski, P., Ryl, J., 2022. The role of electrolysis and enzymatic hydrolysis treatment in the enhancement of the electrochemical properties of 3D-printed carbon black/poly(lactic acid) structures. Appl. Surf. Sci. 574, 151587 https://doi.org/10.1016/j.apsusc.2021.151587.

Kunuku, S., Ficek, M., Wieloszynska, A., Tamulewicz-Szwajkowska, M., Gajewski, K., Sawczak, M., Lewkowicz, A., Ryl, J., Gotszalk, T., Bogdanowicz, R., 2022. Influence of B/N co-doping on electrical and photoluminescence properties of CVD grown homoepitaxial diamond films. Nanotechnology 33, 125603. https://doi.org/10.1088/1361-6528/ac4130.

Le, T.X.H., Charmette, C., Bechelany, M., Cretin, M., 2016. Facile preparation of porous carbon cathode to eliminate paracetamol in aqueous medium using electro-fenton system. Electrochim. Acta 188, 378–384. https://doi.org/10.1016/j.electacta.2015.12.005.

Le, T.X.H., Nguyen, T.V., Amadou Yacouba, Z., Zoungrana, L., Avril, F., Nguyen, D.L., Petit, E., Mendret, J., Bonniol, V., Bechelany, M., Lacour, S., Lesage, G., Cretin, M., 2017. Correlation between degradation pathway and toxicity of acetaminophen and its by-products by using the electro-Fenton process in aqueous media. Chemosphere 172, 1–9. https://doi.org/10.1016/j.chemosphere.2016.12.060.

Liu, Y., Fan, X., Quan, X., Fan, Y., Chen, S., Zhao, X., 2019. Enhanced perfluorooctanoic acid degradation by electrochemical activation of sulfate solution on B/N codoped diamond. Environ. Sci. Technol. 53, 5195–5201. https://doi.org/10.1021/acs.est.8b06130.

López Zavala, M.Á., Jaber Lara, C.R., 2018. Degradation of paracetamol and its oxidation products in surface water by electrochemical oxidation. Environ. Eng. Sci. 35, 1248–1254. https://doi.org/10.1089/ees.2018.0023.

Lu, W., Xu, P., Shao, S., Li, T., Zhang, H., Li, X., 2021. Multifunctional carbon felt electrode with N-rich defects enables a long-cycle zinc-bromine flow battery with ultrahigh power density. Adv. Funct. Mater. 31, 2102913 https://doi.org/10.1002/adfm.202102913.

Marques, S.C.R., Marcuzzo, J.M., Baldan, M.R., Mestre, A.S., Carvalho, A.P., 2017. Pharmaceuticals removal by activated carbons: role of morphology on cyclic thermal regeneration. Chem. Eng. J. 321, 233–244. https://doi.org/10.1016/j.cej.2017.03.101.

Moctezuma, E., Leyva, E., Aguilar, C.A., Luna, R.A., Montalvo, C., 2012. Photocatalytic degradation of paracetamol: intermediates and total reaction mechanism. J. Hazard Mater. 243, 130–138. https://doi.org/10.1016/j.jhazmat.2012.10.010.

Niedziałkowski, P., Bojko, M., Ryl, J., Wcisło, A., Spodzieja, M., Magiera-Mularz, K., Guzik, K., Dubin, G., Holak, T.A., Ossowski, T., Rodziewicz-Motowidło, S., 2021. Ultrasensitive electrochemical determination of the cancer biomarker protein sPD-L1 based on a BMS-8-modified gold electrode. Bioelectrochemistry 139, 107742. https://doi.org/10.1016/j.bioelechem.2021.107742.

Noh, T.H., Kim, M.Y., Kim, D.H., Yang, S.H., Lee, J.H., Park, H.S., Noh, H.S., Lee, M.S., Kim, H.S., 2017. Electrochemical studies of carbon felt electrode modified under airless conditions for redox flow batteries. J. Electrochem. Sci. Technol 8, 155–161. https://doi.org/10.33961/JECST.2017.8.2.155.

Orimolade, B.O., Zwane, B.N., Koiki, B.A., Rivallin, M., Bechelany, M., Mabuba, N., Lesage, G., Cretin, M., Arotiba, O.A., 2020. Coupling cathodic electro-fenton with anodic photo-electrochemical oxidation: a feasibility study on the mineralization of paracetamol. J. Environ. Chem. Eng. 8, 104394 https://doi.org/10.1016/j.jece.2020.104394.

Ortiz-Ortega, E., Hosseini, S., Martinez-Chapa, S.O., Madou, M.J., 2021. Aging of plasma-activated carbon surfaces: challenges and opportunities. Appl. Surf. Sci. 565, 150362 https://doi.org/10.1016/j.apsusc.2021.150362.

Periyasamy, S., Muthuchamy, M., 2018. Electrochemical oxidation of paracetamol in water by graphite anode: effect of pH, electrolyte concentration and current density. J. Environ. Chem. Eng. 6, 7358–7367. https://doi.org/10.1016/j.jece.2018.08.036.

Rahmani, A., Seid-mohammadi, A., Leili, M., Shabanloo, A., Ansari, A., Alizadeh, S., Nematollahi, D., 2021. Electrocatalytic degradation of diuron herbicide using three-dimensional carbon felt/β-PbO$_2$ anode as a highly porous electrode: influencing factors and degradation mechanisms. Chemosphere 276, 130141. https://doi.org/10.1016/j.chemosphere.2021.130141.

Ryl, Brodowski, Kowalski, Lipinska, Niedzialkowski, Wysocka, 2019. Corrosion inhibition mechanism and efficiency differentiation of dihydroxybenzene isomers towards aluminum alloy 5754 in alkaline media. Materials 12, 3067. https://doi.org/10.3390/ma12193067.

Ryl, Burczyk, L., Zielinski, A., Ficek, M., Franczak, A., Bogdanowicz, R., Darowicki, K., 2019. Heterogeneous oxidation of highly boron-doped diamond electrodes and its influence on the surface distribution of electrochemical activity. Electrochim. Acta 297, 1018–1027. https://doi.org/10.1016/j.electacta.2018.12.050.

Smith, R.E.G., Davies, T.J., Baynes, N. de B., Nichols, R.J., 2015. The electrochemical characterisation of graphite felts. J. Electroanal. Chem. 747, 29–38. https://doi.org/10.1016/j.jelechem.2015.03.029.

Sobaszek, M., Siuzdak, K., Sawczak, M., Ryl, J., Bogdanowicz, R., 2016. Fabrication and characterization of composite TiO$_2$ nanotubes/boron-doped diamond electrodes towards enhanced supercapacitors. Thin Solid Films 601, 35–40. https://doi.org/10.1016/j.tsf.2015.09.073.

Tian, M.-J., Liao, F., Ke, Q.-F., Guo, Y.-J., Guo, Y.-P., 2017. Synergetic effect of titanium dioxide ultralong nanofibers and activated carbon fibers on adsorption and photodegradation of toluene. Chem. Eng. J. 328, 962–976. https://doi.org/10.1016/j.cej.2017.07.109.

Vieno, N., Tuhkanen, T., Kronberg, L., 2007. Elimination of pharmaceuticals in sewage treatment plants in Finland. Water Res. 41, 1001–1012. https://doi.org/10.1016/j.watres.2006.12.017.

Wallart, X., Henry de Villeneuve, C., Allongue, P., 2005. Truly quantitative XPS characterization of organic monolayers on silicon: study of alkyl and alkoxy monolayers on H−Si(111). J. Am. Chem. Soc. 127, 7871–7878. https://doi.org/10.1021/ja0430797.

Wang, M., Simon, N., Decorse-Pascanut, C., Bouttemy, M., Etcheberry, A., Li, M., Boukherroub, R., Szunerits, S., 2009. Comparison of the chemical composition of boron-doped diamond surfaces upon different oxidation processes. Electrochim. Acta 54, 5818–5824. https://doi.org/10.1016/j.electacta.2009.05.037.

Wu, S., Zhang, L., Chen, J., 2012. Paracetamol in the environment and its degradation by microorganisms. Appl. Microbiol. Biotechnol. 96, 875–884. https://doi.org/10.1007/s00253-012-4414-4.

Xue, A., Yuan, Z.-W., Sun, Y., Cao, A.-Y., Zhao, H.-Z., 2015. Electro-oxidation of perfluorooctanoic acid by carbon nanotube sponge anode and the mechanism. Chemosphere 141, 120–126. https://doi.org/10.1016/j.chemosphere.2015.06.095.

Zhong, S., Padeste, C., Kazacos, M., Skyllas-Kazacos, M., 1993. Comparison of the physical, chemical and electrochemical properties of rayon- and polyacrylonitrile-based graphite felt electrodes. J. Power Sources 45, 29–41. https://doi.org/10.1016/0378-7753(93)80006-B.

Zhou, J., Zhang, Y., Balda, M., Presser, V., Kopinke, F.-D., Georgi, A., 2022. Electro-assisted removal of polar and ionic organic compounds from water using activated carbon felts. Chem. Eng. J. 433, 133544 https://doi.org/10.1016/j.cej.2021.133544.

Zhou, L., Zhou, M., Hu, Z., Bi, Z., Serrano, K.G., 2014. Chemically modified graphite felt as an efficient cathode in electro-Fenton for p-nitrophenol degradation. Electrochim. Acta 140, 376–383. https://doi.org/10.1016/j.electacta.2014.04.090.

Zhu, M., Kong, L., Xie, M., Lu, W., Liu, H., Li, N., Feng, Z., Zhan, J., 2021. Carbon aerogel from forestry biomass as a peroxymonosulfate activator for organic contaminants degradation. J. Hazard Mater. 413, 125438 https://doi.org/10.1016/j.jhazmat.2021.125438.

Zielinski, A., Cieslik, M., Sobaszek, M., Bogdanowicz, R., Darowicki, K., Ryl, J., 2019. Multifrequency nanoscale impedance microscopy (m-NIM): a novel approach towards detection of selective and subtle modifications on the surface of polycrystalline boron-doped diamond electrodes. Ultramicroscopy 199, 34–45. https://doi.org/10.1016/j.ultramic.2019.01.004.